EAI Endorsed Transactions
on Energy Web
Research Article EAI.EU

Optimized design and application of slot-type solar concentrator based on BIM technology

Miaoling Wang*, Hao Wang

School of Construction Management, Chongqing Metropolitan College of Science and Technology, Chongqing, 402160, China

Abstract

In recent years, the application of Building Information Modeling (BIM) technology in the construction industry has significantly improved design efficiency and reduced energy consumption, and its application in other design fields has gradually received attention. However, in traditional solar collector designs, steel consumption and production costs are high, and effective optimization methods are still lacking. The research aims to apply BIM technology to save steel in the design of solar collectors, thereby reducing production costs and meeting the dual requirements of energy efficiency and cost-effectiveness. Compared with traditional design methods, BIM technology can optimize the design process and reduce unnecessary material waste through precise modeling and analysis. To achieve this goal, this study conducted static analysis and steel minimization planning analysis by constructing a finite element model (FEM) of a solar collector. The specific method is to first use BIM technology to establish a 3D model of the collector, then conduct structural static analysis, and finally evaluate and optimize the steel usage through multiple linear regression algorithm. The experimental data comes from model analysis of actual collector structures and is validated using standard physical and engineering calculation methods. The results showed that in the optimized design *02 scheme, the steel consumption was significantly reduced, with a total steel consumption of 805.962kg and a steel cost of 3974.9 yuan, a decrease of 10.99% compared to the pre optimized 4465.5 yuan. The maximum displacement and maximum stress of this scheme, although slightly higher than other schemes, are still far below the allowable values of the structure. It has the best comprehensive optimization effect while ensuring safety. These achievements indicate that the application of BIM technology can not only effectively reduce the steel consumption of solar collectors, but also lower production costs, and has strong practical application value. This provides useful reference and practical guidance for optimizing the design of other similar devices in promoting the design of renewable energy equipment.

Key words: BIM technology, Trough condenser, Steel consumption, Structural stress, Mirror displacement, solar energy, Structural design

Received on 19 September 2024, accepted on 18 April 2025, published on 11 June 2025

doi: 10.4108/ew.7308

*Corresponding author. Email: wangmiaoling2022@163. com

1. Introduction

With the continuous advancement of technology, the importance of trough solar concentrators in the development of renewable energy is further highlighted [1]. However, research on trough solar concentrators mainly focuses on optimizing optical efficiency or thermal performance, often overlooking the potential for reducing material costs through structural design. Traditional design methods rely on iterative physical prototypes and manual calculations, which are time-consuming, lack interdisciplinary collaboration, and cannot systematically combine structural analysis with cost optimization [2]. The application of BIM technology in the fields of architecture and infrastructure design has gradually matured, and its established design models can organically combine all project participants to achieve collaborative design [3]. Although BIM technology has been widely used in architectural design, it has not yet been widely applied in the design of solar concentrators for structural optimization and material savings. How to use BIM technology to optimize the design of trough solar concentrators, reduce production costs, and save materials is still an unsolved problem. Therefore, this study innovatively applies BIM technology to the optimization design of steel volume for solar concentrator manufacturing, in order to avoid or reduce the problems of low efficiency and poor collaboration that may be faced in traditional design processes. At the same time, the FEM of the concentrator was designed, combined with BIM technology and static analysis, and the structural optimization evaluation indicators were reasonably calculated through multiple linear regression algorithm, achieving dual optimization of steel consumption and steel cost. This will help provide new ideas for optimizing the design of solar energy equipment and promote the development of China's solar power generation industry.

2. Related works

In recent years, the optimization design of solar trough concentrators has been a research hotspot. Many scholars focus on improving optical efficiency and thermal performance. For example, Gong J et al. used an innovative design method of the secondary reflector, which was formed based on an adaptive approach to maximize the portion of solar radiation reflected by the primary reflector but not captured back to the absorber tube, compared with no optimized reflector, the former optical efficiency improved by 5.2% [3]. Zhang et al. found disadvantages of parabolic trough solar concentrator systems in connecting receiver tube components and increasing the concentration ratio. To overcome these inherent drawbacks, an innovative concept of a linearly focused secondary trough concentrating system is proposed in this paper and the optical evaluation results show that this innovative solar concentrating system has a high application value as a solar experimental device [4]. This type of research focuses on improving optical and thermal efficiency, however, there is relatively little research on material savings and cost optimization. Some studies have focused on the design of trough concentrators from an economic perspective, such as, Widjaja et al. analyzed the possibility of combining a trough solar system with a concrete warehouse for process heating applications. The results found that this design scheme effectively reduces the industrial operation cost of pasteurization process heating [5]. Zhou et al. proposed a compact solar collector with integrated prisms and semi-parabolic trough mirrors for efficient solar energy collection in a limited space. It was found that this improved solar collector effectively improves the solar thermal efficiency of the facility, providing a more practical application and economically feasible scheme for faster and more convenient practical solar energy for buildings [6]. However, the application of BIM technology is still relatively limited in these optimized designs.

Traditional design methods rely on physical prototypes and manual calculations, which suffer from inefficiencies and lack of interdisciplinary collaboration. The introduction of BIM technology has provided new solutions for interdisciplinary collaboration, but currently most research is still limited to optimizing single design parameters such as optical efficiency or thermal performance. Dugaria et al. found that the addition of nanoparticles to the base fluid can enhance its optical properties, especially its absorption properties. That is, nanofluids can be used in solar collectors to absorb solar radiation in their structures. Therefore, the authors investigated the application of aqueous suspensions as bulk absorbers in concentrated direct absorption solar collectors and selected single-walled carbon nano-horn suspensions as nanofluids. A model of a planar geometry solar receiver installed in a parabolic trough concentrator was developed and the results of the study showed that the simulated performance of the direct absorption receiver would be better than that of two surface absorption conventional receivers under the same operating conditions [7]. Gang proposed a novel concentrated PV/thermal system based on a parabolic trough concentrator and an indium tin oxide glycol nanofluid spectral filter. The results of thermodynamic analysis showed that the theoretical photovoltaic conversion efficiency and solar thermal efficiency of the system were 29. 1% and 17. 2%, respectively, which were higher than those of the compared conventional system [8]. Mihaa found that due to the inherent complexity of nanofluidic systems, including the interactions between the optical and thermophysical properties of each phase, the development and optimization of solar energy absorption and storage systems in nanofluid-based receivers requires advanced mathematical physical models for more efficient design and optimization. This study evaluates the impact of these key assumptions on predicting the thermal absorption and thermal energy storage capacity of such systems and developing accurate predictive models to aid the design and optimization of such systems [9]. These studies provide new optimization ideas for solar collectors, but most of them do not consider how BIM technology can optimize the structure and reduce material consumption in the design process.

In summary, many studies have been conducted by professional scholars in the industry to improve the construction efficiency and solar energy utilization efficiency of solar equipment, but most of them failed to consider the use of BIM technology for collaborative design and only started to improve the design structure of the solar equipment itself, which plays an important role in improving the scientific nature of the design results and reducing design process errors. Therefore, this study attempts to apply BIM technology to the optimal design of trough solar concentrators.

3. Optimized design of trough solar concentrator combined with BIM technology

3. 1 Co-design of trough solar concentrator integrating BIM technology

Collaborative design can cope with the design conflicts brought about by different types of designers working in teams, designers can work together under a unified platform and communicate in a timely manner [10]. The emergence of BIM technology has brought great reform to the traditional design method based on CAD files [11]. Using BIM technology for design, the project can no longer be displayed only on a two-dimensional plane, which can better express the design intent, and different designers can participate in the project design process at the same time to achieve efficient co-working [12]. With the use of BIM technology, projects can no longer only be displayed on a two-dimensional plane, which can better express the design intention, and different designers can participate in the design process at the same time to realize efficient collaboration [13]. Specifically, the difference between the traditional design process based on CAD 2D files and the collaborative design process based on BIM technology can be shown in Figure 1. Note that the dotted line in Figure 1 represents the steps with the same meaning in the two design processes, which are marked for comparison and observation.

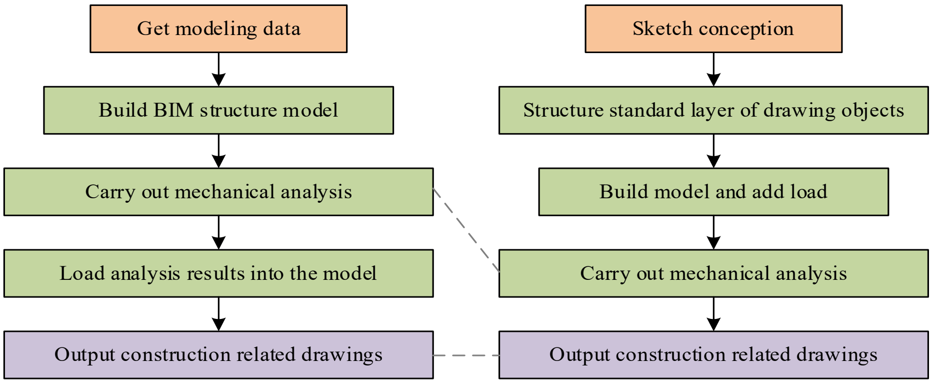

（a）Design process based on BIM technology

（b）Design process based on traditional two-dimensional technology

Figure 1 Comparison of the design process based on BIM technology and CAD 2D files

Traditional CAD software can also create 3D models. However, there are significant differences between traditional CAD and BIM 3D modeling in terms of design functionality, parametric modeling, and automatic change synchronization [14]. As shown in Table 1, the BIM 3D model can realize the function of automatic statistics of construction materials to provide a reference for subsequent construction, and also facilitate the collision check of the model, and there is an obvious logical relationship between the model and the plan construction drawings generated by it [15]. Currently, most domestic units still use the traditional method to design solar concentrators, but this method cannot plan the functions of the concentrator from a holistic perspective, nor can it integrate the needs of various professions, thus making the finished products produced cannot well meet the different needs of use. BIM technology is applicable to assist in the optimal design of this trough solar concentrator.

Table 1 The difference between traditional technology and BIM technology 3D modeling comparison

Comparison Items	Traditional space building modeling	BIM technology spatial building modeling	Explanation
Design function	Space display map	Space display drawings, design, management, mechanical analysis, etc.	Both also support virtual reality technology applications
Model Parametric Design	Not supported	Support	Exact parameters need to be given
Automatic modification	Not supported	Support	A small number of core parameters need to be given
Collaborative Office Efficiency	Relatively lower	Relatively higher	Co-working for different professionals
Relationship to floor plans	Weak correlations	Logical correspondence, can automatically be modified together	/

In the process of using BIM technology to carry out collaborative design, to promote the project in an orderly manner, the design of each profession should conform to an overall workflow, and the design of the trough solar concentrator also needs to follow this process, as shown in Figure 2.

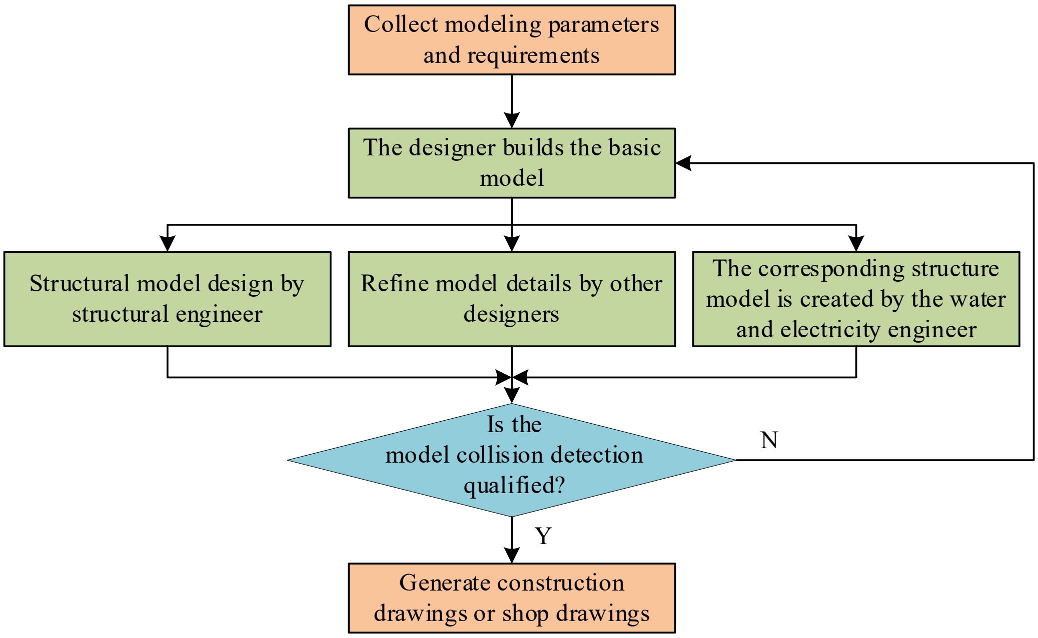

Figure 2 General workflow of collaborative design based on BIM technology

According to the analysis of Figure 2, BIM technology can be applied to the following steps in the design of slot-type solar concentrator, determining the design objectives of the concentrator, establishing a collaborative work platform, assisting in carrying out collision inspection, statistics and calling material information, and producing design drawings, and the application of these aspects is explained in detail below. In terms of establishing a collaborative work platform, considering the need for solar radiation analysis of concentrators and simulation of real working conditions, Ecotect Analysis software was selected as the BIM modeling tool. Combining Revit Architecture features to render the concentrator model with high realism, simulating the state under sunlight, and assisting in expressing design intent. Considering the efficiency of the concentrator to receive solar radiation, it is better to place the concentrator model in the form of a north-south direction. In terms of collision check fees, the model built with Tekla Structures can significantly reduce the design changes caused by collisions, and even if there are design changes, only minimal modifications are required, and the parts associated with them will be automatically changed and adjusted. Tekla Structures also provides a detailed description of the material usage of the concentrator, which is stored in the public platform and can be easily called up by the manufacturer, and helps reduce unnecessary development costs. development costs. In terms of drawing, using a BIM model to carry out the drawing work can simplify the model visualization and coordination in the design stage, and help the owner to generate material statistics, collision detection reports, etc. In addition, the model structure detail drawings constructed by using BIM technology can be integrated with traditional design drawings, thus reducing the difficulty of reading, and understanding for people with poor professional backgrounds.

3. 2 Construction of structural optimization model of trough solar concentrator

There is a correlation between the structure of the trough solar concentrator and the amount of steel used, and its manufacturing cost often accounts for more than half of the overall system cost. Therefore, it is of practical significance to optimize the structure of the concentrator and reduce the manufacturing cost under normal operating conditions. In this study, the dimensions of the pull fin and the main triangular truss are simplified as continuous parameters, and the initial tension of the latch is considered a qualitative parameter. Different test points are used to represent different experimental schemes, and then MIDAS software is used for static analysis to ensure that the optimized concentrator designed meets the mechanical requirements. In order to simplify the calculation process and amount in the design process, some parameters and structural data are predicted by algorithms, so it is necessary to select a more accurate regression algorithm to perform this step. Finally, the BIM model established by Tekla Structures is used to count the quantity, size, model, quality, and other properties of steel required for the structure, so as to verify the feasibility of reducing the cost of the condenser structure. The following is the design of the regression calculation process in the study. This study implemented regression analysis of a multiple linear regression model using MATLAB R2018a software. Multiple linear regression has fast calculation speed and is suitable for real-time optimization loops embedded in BIM platforms. The general expression of the multiple linear regression model is shown in formula (1),

$$Y_t = \beta_1 + \beta_2 X_{2t} + \ldots + \beta_k X_{kt} + u_1 \quad (1)$$

Where β_k represents the regression coefficient, represents the X_{jt} t th response value of the j th independent variable X_j in the model. u_t represents the random variable, and Y_t is the predicted value of the t regression in the dependent variable Y. The coefficients of multiple linear regression directly reflect the degree of influence of each design variable on the objective, making it easier for engineers to understand and guide design adjustments. In this study, $\overline{R}^2$ is the coefficient of determination of the modified degrees of freedom, was selected as an indicator to evaluate the fit of the multiple linear regression model, and the method of calculation of the indicator is more common and will not be repeated here. In addition, the F-statistic was selected in this study as an indicator to verify the significance of the regression equation, i.e. , to evaluate the level of closeness of the relationship between the dependent variable and the respective variable.

After completing the regression model selection and using the step design, then design the FEM of the trough solar concentrator, which is a solar thermal power generation device that can collect solar energy on the collector tube for subsequent devices to convert solar energy into electricity [16]. Trough solar concentrators are generally installed in areas with abundant solar energy and little shading, but the wind load in these areas is also greater. Excessive wind load will cause the mirror surface of the concentrator to deform beyond the design value, thus reducing the efficiency of the device to collect solar energy [17-18]. The common condenser structure is shown in Figure 3. The left figure in Figure 3 shows the internal truss structure of the top facility of the condenser, and the right figure shows the elevation of the whole condenser.

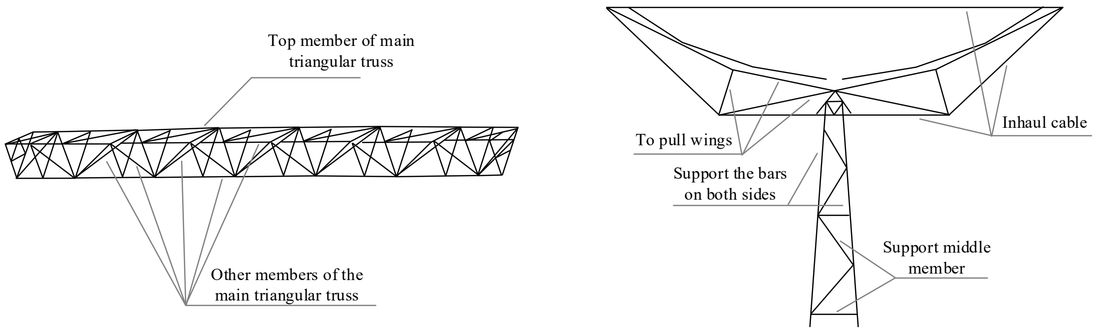

Figure 3 Sketch of common concentrator structure

It can be seen from Figure 3 that when the mirror surface of the concentrator and the ground are at an angle of 90 degrees, the body coefficient of the concentrator achieves the maximum value, which is the most unfavorable working condition, and the subsequent optimization is based on this working condition. The angle of the concentrator mirror under this working condition can be expressed in the sketch shown in Figure 4.

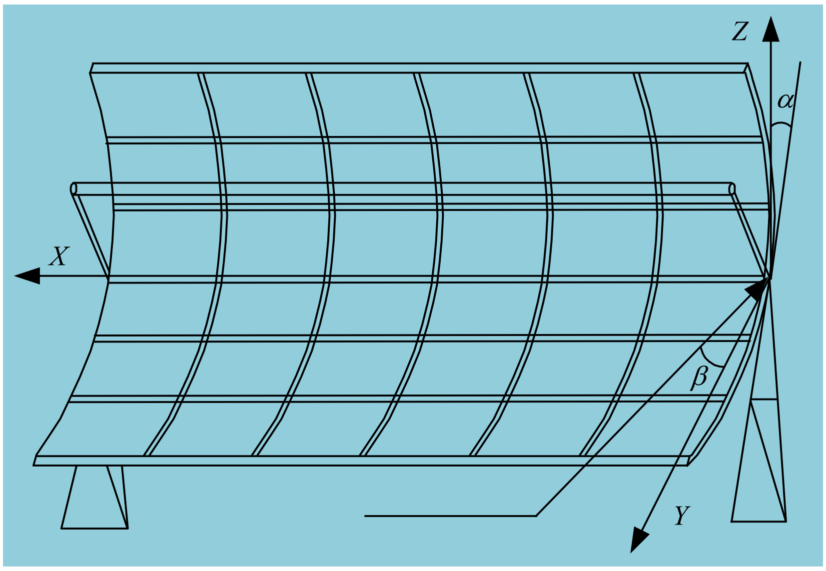

Figure 4 Sketch of concentrator lens angle under the most unfavorable working conditions

The FEM of the slotted concentrator was then designed according to the state of Figure 4. The concentrator device selected for this study consists of six rows and six columns layout of mirror plate, pulling fins, pulling cables, main triangular truss, and bottom support, in which the pulling locks use 6. 2 mm diameter, 1270 MPa strength steel strand, and the constituent materials of bracket and mirror are Q235 steel and common soda lime glass, respectively, whose elastic modulus, Poisson's ratio, and density are 206E/GPa vs. 73E/GPa, 0. 3 vs. 0. 3 vs. 0. 2, 7860Kg-m-3 , 2550Kg-m-3 [19-21]. Compared with the superstructure, the concrete base stiffness model of the slot type concentrator is larger, and it is treated as a fully solidified form in the FEM [22]. Then set the tension fin and mirror plate, bottom support and main triangle truss are rigid connection, and the plate end restraint release treatment. Then analyze the load on the FEM. Considering that the stiffness of the concentrator structure is large, the main frequency of wind load is very similar to the self-oscillation frequency it brings, so the wind load on the enclosure structure in the Code for Structural Loads of Buildings (GB50009-2012) is used to calculate the wind load here, and the formula is shown in equation (2) [23-24].

$$w_k = \beta_{gz}\mu_{s1}u_z w_0 \quad (2)$$

In equation (2) w_k represents the wind load on the concentrator, β_{gz} is the gust coefficient at the height of z position, μ_{s1} is the local wind pressure coefficient of the mirror plate that will be 10 m height as the reference point, and u_z represents the variation parameter of the wind pressure height[25]. w_0 The basic wind pressure at the facility location is taken as the maximum wind speed more commonly encountered at the spotting mirror facility, i.e., 0. 12 KPa for a wind speed of 6. Also, since the spotting mirror in the study is assumed to be placed in the B interior landscape with a maximum height of less than 10 m, the values of the above parameters can be obtained by checking the table at $\beta_{gz} = 1.7$ and $u_z = 1.0$. However, because the structure of the spotting scope is more complicated, μ_{s1} needs to be obtained through wind tunnel experiments [26]. In the wind tunnel experiment, the same position of the front and back of the spotting scope is chosen as the arrangement of measurement points, and the net wind pressure coefficient C_{Pi} of each measurement point is calculated using equation (3).

$$C_{Pi} = \frac{2\left(P_i^f(t) - P_i^b(t)\right)}{\rho V_H^2} \quad (3)$$

Where i represents the measurement point number, $P_i^f(t)$ and $P_i^b(t)$ represent the corresponding wind pressure on the upper and lower surfaces of the double-sided measurement points, ρ is the test air density, and V_H represents the wind speed at the reference point. In order to analyze the wind pressure on the mirror surface more intuitively, the mirror surface is partitioned by the principle that the average wind pressure coefficients among all measurement points in the same partition do not have alternating positive and negative variations, and the average wind pressure coefficient of each partition $\bar{C}_{Pj,mean}$ is calculated according to equation (4).

$$\bar{C}_{Pj,mean} = \frac{\sum \bar{C}_{Pi,mean} A_i}{\sum A_i} \quad (4)$$

Where j is the number of the partition, $\bar{C}_{Pi,mean}$ is the average wind pressure coefficient of the measurement point within the i j partition, A_i is the area belonging to the measurement point i within the j partition, and $\sum A_i$ is the sum of the area belonging to the measurement point i within the partition. For Class B landforms, if the equipment is located at a height lower than 12 m, the body coefficient of each partition will be consistent with its corresponding regional average wind pressure coefficient, but considering that the height of the mirror plate is less than 10 m, there exists equation (5).

$$\mu_{s1}(j) = \bar{C}_{Pj,mean} \quad (5)$$

Then construct the optimization model of the steel consumption of the concentrator, which is essentially an optimization problem with the objective function of minimizing the steel consumption also i.e. $Min\ G(m_1, m_2, m_3, m_4)$, m_1, m_2, m_3, m_4 are the parameters involved in the optimization process, which represent the cross-sectional outer diameter of rod No. 1, the cross-sectional outer diameter of rod No. 2, the cross-sectional limb width of rod No. 3, and the initial stress of the lasso, respectively. The three parameters m_1 , m_2 and m_3 directly affect the structural rigidity, steel consumption, and mechanical properties of the concentrator. By adjusting the dimensions of the rods, the balance between material consumption and structural safety can be optimized. m_4 is a key factor in controlling structural deformation, and its presence and magnitude significantly affect the dynamic stability of the concentrator. The constraints of the optimization model need to consider the range of values of each parameter, the maximum stresses to which the structure is subjected, with and without the initial stresses of the ties, from which the constraints of the optimization model can be obtained, as shown in equation (6).

$$\begin{cases} \sigma_{\max} < 215MPa \\ W_{\max} < W_{\lim} \\ 50mm < m_1 < 60mm \\ 39mm < m_2 < 54mm \\ 36mm < m_3 < 46mm \\ 0 < m_4 < 1 \\ m_1, m_2, m_3, m_4 \in N^* \end{cases} \quad (6)$$

Where W_{max} , W_{lim} represent the maximum displacement produced by the mirror structure of the concentrator and the maximum displacement that can be withstood, respectively. After FEM calculations, it is known that the maximum displacement of the concentrator mirror selected is 16. 244mm when both the horizontal and vertical angles are 0°, so this value is set as W_{lim} . m_1, m_2, m_3 The limits of the product are set with reference to the data of similar products in the market.

4. Analysis of optimized design results of slot-type solar concentrator

4. 1 Simulation analysis experimental scheme and parameter design

In this simulation analysis experiment, the poles 1, 2 and 3 of the concentrator are steel round tubes with thickness of 4mm, 2. 5mm and angles with thickness of 3mm respectively, while the cross section of pole 4 is made of rectangular steel tube with size $60 \times 30 \times 2$ and pole 5 is made of rectangular steel tube with cross section size $30 \times 20 \times 1.5$. In addition, considering the structure and size of the common slot type concentrator in the market, the opening size, column height and length of the concentrator of the research object are set to 6m, 3. 2m and 6. 1m respectively, and the shape of the curved surface of the concentrator conforms to the parabolic equation $x^2 = 8000y$.

Considering that the uniform design table used in this study was designed according to the number of levels of 6, so the corresponding number of levels of the initial tension of the lasso was also fixed to 6 here, and the states with and without the initial tension appeared three times in the experiment respectively, so the parameter level table could be collated as shown in Table 2.

Table 2 Table of parameter levels of the FEM of the concentrator

Experimental protocol number	Parameters m_1 (mm)	Parameters m_2 (mm)	Parameters m_3 (mm)	Parameters m_4 (KN)
#01	49. 0	38. 0	35. 0	≠0
#02	51. 0	41. 0	37. 0	≠0
#03	53. 0	44. 0	39. 0	≠0
#04	55. 0	47. 0	41. 0	0
#05	57. 0	50. 0	43. 0	0
#06	59. 0	53. 0	45. 0	0

In this study, $U_{18}\left(6^4\right)$ from the uniform design table was chosen to carry out the experiments, and the maximum stress value of steel σ_{max} , the amount of steel used G , and the maximum displacement of the mirror W_{max} were used as indicators to evaluate the safety of the concentrator device. Map the horizontal values of the parameters in Table 2 to the specific parameters according to the sequence numbers (N_1 - N_4) of the uniform design table $U_{18}\left(6^4\right)$, and obtain Table 3.

In Table 3, the horizontal values of each parameter appeared uniformly in 18 experiments, and the combination between parameters satisfied the spatial filling characteristics to avoid correlation interference. For example, in Experiment number 1, N_1 =3 corresponds to m_1 =53mm (m_1 of the #03 in Table 2), and N_4 =6 corresponds to m_4 =0 (m_4 of the #06 in Table 2). This method involves 18 experiments covering a combination of multiple parameters and levels, balancing efficiency and scientificity.

Table 3 List of test protocols

Experiment number	Parameters m_1 (mm)	Parameters m_2 (mm)	Parameters m_3 (mm)	Parameters m_4 (KN)	N_1	N_2	N_3	N_4
1	53	41	39	0	3	2	3	6
2	51	38	45	≠0	2	1	6	3
3	55	50	45	≠0	4	5	6	1
4	53	53	35	≠0	3	6	1	2
5	53	47	43	0	3	4	5	4
6	55	38	41	0	4	1	4	5
7	51	44	41	≠0	2	3	4	1
8	57	53	39	0	5	6	3	4
9	49	47	39	≠0	1	4	3	2
10	59	41	43	≠0	6	2	5	2

11	55	44	37	≠0	4	3	2	3
12	59	50	41	≠0	6	5	4	3
13	57	44	45	0	5	3	6	6
14	49	41	35	0	1	2	1	4
15	57	38	37	≠0	5	1	2	1
16	49	53	43	0	1	6	5	5
17	59	47	35	0	6	4	1	5
18	47	50	37	0	2	5	2	6

4. 2 Analysis of simulation experiment results

Use 0-1 variable to quantitatively describe the qualitative variables in the experiment, and use correlation coefficient and determination coefficient to describe the fitting degree of the regression equation, and carry out the F difference significance test. The significance level is set as 0. 05. After the static analysis based on the FEM is completed, Figure 5 is obtained. Note that to compare the reliability of the multiple linear regression model selected in this study, XGBoost algorithm commonly used in regression analysis is selected for the same regression operation. Based on the analysis in Figure 5, the maximum displacement and predicted average absolute error (MAE) of XGBoost algorithm for steel usage are 4.59% ± 0.81% and 4.68% ± 0.98%, respectively. For maximum displacement prediction, the MAE of the multiple linear regression model is 1.36% ± 0.21%, while the steel consumption error is 1.75% ± 0.18%, indicating its strong predictability. The correlation coefficients are higher than 0. 90, and the P value of F test is less than 0. 05. It can be seen that the regression effect of the multiple linear regression model selected in this study is slightly different from that of the XGBoost regression model, and the error between the model and the test value is also small. The fitting effect is good, but the former has greater advantages in computing speed and interpretability. It can be seen that the use of multi-dimensional linear model to describe the four experimental parameters, the maximum displacement of the condenser mirror and the total amount of structural steel in this study is more reasonable, and it can be seen from Table 3 that there is a negative linear correlation and a positive linear correlation between the former and the latter respectively. That is to say, with the increase of test parameters, the maximum displacement of the condenser mirror will decrease as a whole, and whether there is an initial cable tension in the structure has a significant impact on this index. At this time, the total amount of structural steel will also increase, but the total amount of structural steel is almost not affected by the initial cable tension, but more likely to be affected by the main beam truss and fins.

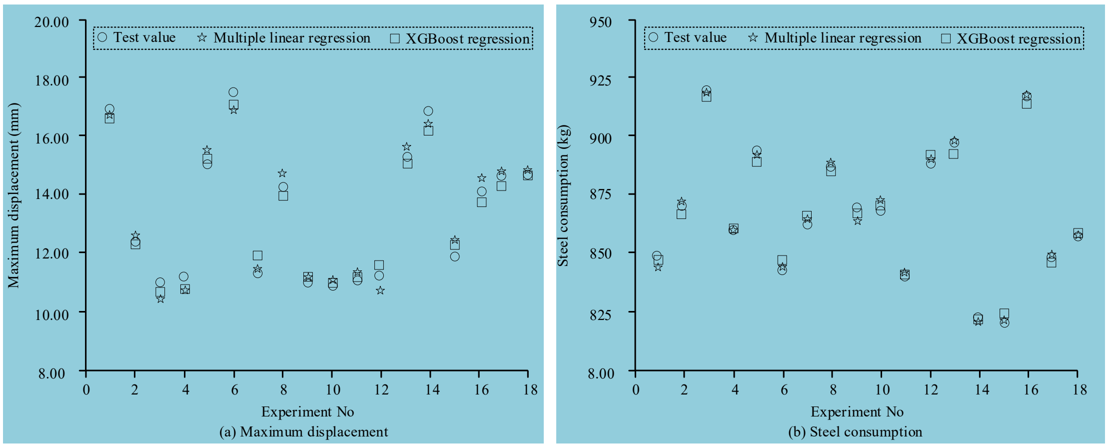

Figure 5 Fit of model regression values to experimental values

After completing the calculation of the optimized model for the structural steel consumption, the statistical results are obtained in Figure 6 and Figure 7, which are used to show the mechanical evaluation indexes maximum displacement and maximum stress, as well as the economic indexes steel consumption and steel cost for the optimal scheme set, respectively. Note that the corresponding parameter values of each scheme in the horizontal axis in Figure 6 are shown in Table 4. The parameter names in the table have the same meanings as those in Table 2 and Table 3.

Table 4 Correspondence table of parameter values for the optimal scheme set

Optimal scheme number	Parameters m_1 (mm)	Parameters m_2 (mm)	Parameters m_3 (mm)	Parameters m_4 (KN)
*01	51	37	35	1
*02	49	38	35	1
*03	50	39	35	1
*04	54	37	35	1
*05	49	38	34	1
*06	52	38	34	1
*07	48	39	34	1

Observing Figure 6, it can be seen that the maximum displacement indicator of the mirror of the concentrator is sensitive to the parameter m_2, which is the outer diameter of the cross-section of the No. 2 rod, and when the value of this parameter is low, the value of the maximum displacement indicator is higher, and vice versa, the value decreases. For example, the maximum displacement of the mirror surface of the concentrator is 11. 954mm and 11. 983mm when the maximum value of the parameter m_2 is 39mm in *03 and *07, respectively. But the maximum displacement of the mirror surface is not sensitive to the parameter m_1. As for the maximum stress, the maximum stress of each scheme in the steel optimal scheme set is around 12. 000 MPa, and scheme *03 corresponds to the smallest maximum stress index of 11. 954 MPa. Overall, the maximum mirror displacement and maximum stress of each optimal scheme are significantly lower than the allowable maximum displacement and strength limit of the structure, and scheme *03 is the most excellent, with the smallest maximum mirror displacement of each scheme The maximum structural stress of 182. 462 MPa is only slightly higher than that of 182. 453 MPa for scheme *07.

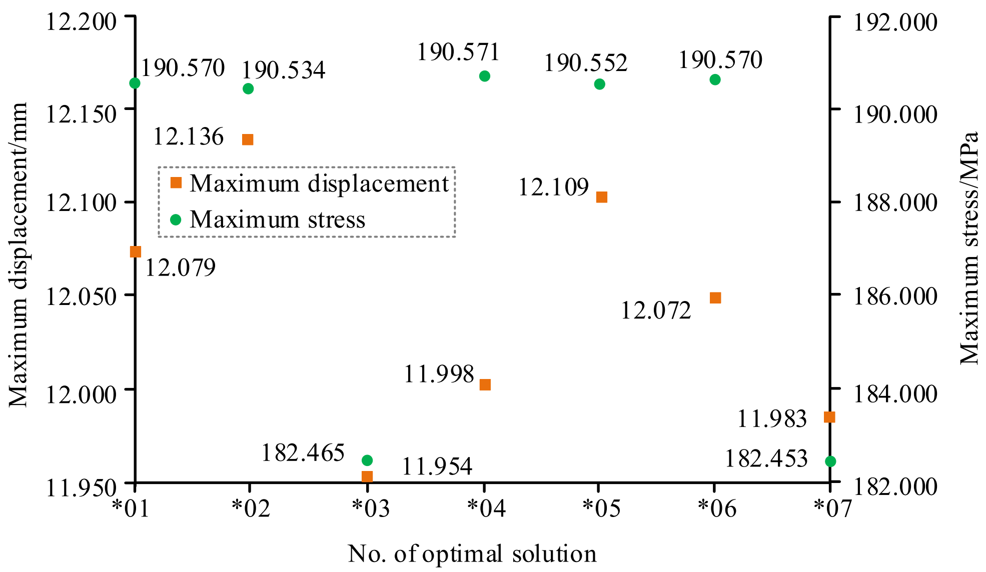

Figure 6 Statistics of mechanical indexes calculated by the optimized model for the amount of steel used in the concentrator

The results of the total structural steel consumption and steel cost indexes for each optimal scheme set are shown in Figure 7, which shows that the differences between the steel consumption and steel cost of each scheme in the optimal scheme set are small. Due to the primary objective of optimization being to minimize the amount of steel used, and the secondary objective being to control stress/displacement within safe thresholds, the steel consumption of the *02 scheme is the lowest among all schemes, only 805.962kg, and the steel cost is also the lowest, only 3974.9 yuan. Its maximum displacement and maximum stress are 12.136mm and 190.534MPa, respectively, which are far below the corresponding allowable values of the structure and will not cause safety issues. The *02 scheme has the best comprehensive optimization effect in this study. By rational layout and reducing material thickness, the structural strength is maintained while reducing steel consumption. Sayyad compared the differences between BIM software and traditional methods in enterprise unit engineering quantity calculation and cost estimation, and the results showed that the total cost estimated by BIM was 1.12% higher than that of traditional methods [27]. This study not only achieves the lowest steel consumption, but also ensures that stress and displacement are strictly below the safety threshold, breaking through the limitations of traditional research that only focuses on a single cost indicator and achieving a balance between lightweight and safety objectives.

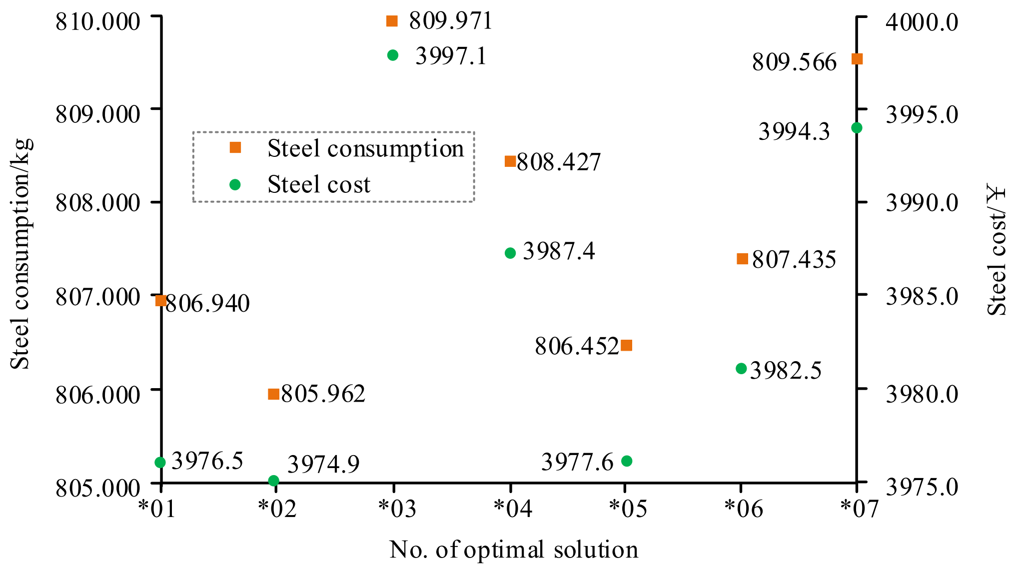

Figure 7 Material index statistics of the results of the optimized model calculation of the amount of steel used in the concentrator

5. Conclusion

BIM technology is an advanced design concept in the civil engineering industry. This study uses BIM technology to optimize the design of trough solar collectors in order to reduce steel consumption during their manufacturing process. At the same time, combined with its FEM to achieve static analysis of equipment structure, a multiple linear regression model is used to verify the amount of consumables. The results showed that the average maximum mirror displacement error and average steel consumption error obtained from the experiment were 4.68% and 1.66% respectively, which are slightly different from the regression prediction value of XGBoost algorithm. The correlation coefficient is greater than 0. 90, and the P value of the F test is less than 0.05. It shows that it is appropriate to use the multiple linear regression algorithm to calculate the optimization evaluation index of the FEM. Comparing different schemes, from the perspective of mechanical indicators, scheme *03 is the best. The maximum displacement of the mirror surface is 11.954mm, which is the minimum for each scheme. The maximum structural stress of 182. 462MPa is only slightly higher than that of Scheme *07, which is 182.453MPa. From the perspective of material indicators, the steel consumption of the *02 scheme is relatively low. Among them, the *02 scheme has the lowest values in terms of total structural steel consumption and steel cost, which are 805. 962kg and 3974.9￥ respectively. The latter is 10. 99% lower than the former condenser steel cost of 4465. 5￥. The maximum displacement and stress of the mirror surface of all alternatives are far lower than the corresponding allowable values of the structure, so in this study, the comprehensive optimization effect of * 02 scheme is the best. The research results show that the application of BIM technology to the design of trough solar concentrators will help to save the materials required to produce equipment and thus play a role in reducing production costs. This is primarily because, By using BIM technology and FEM for precise modeling and analysis of solar trough concentrators, unnecessary redundant structures are eliminated in the early design stage, avoiding a large amount of manufacturing rework or modification, further improving the accuracy and efficiency of the project. Due to the limited experimental conditions, the material and physical properties of each alternative could not be verified by means of actual manufacturing this time. In the future, it is possible to consider manufacturing prototypes of multiple design schemes, verifying steel consumption, production costs, and structural performance through actual testing, to ensure that the economic benefits of design optimization are consistent with theoretical calculations.

Funding

The research is supported by Chongqing Metropolitan College of Science and Technology Reserach Fund for “Research on the Interactive Relationship Between Modular Construction and Low-Carbon Urban Development” (Grant No. CKKY2024022).

Reference

[1] Ebada A, Eltaly B, Tayel M. Advantages of Building Information Modeling Technology (BIM) in Structural Design and Construction Stages. Egypts Presidential Specialized Council for Education and Scientific Research, 2021, 44(4):415-417.

[2] Song A, Cai F, Lei W. Application of BIM Technology in Freezing Design of Metro Section Lateral Pump House. IOP Conference Series: Earth and Environmental Science, 2020, 580 (1):012017-012022.

[3] Gong J, Wang J, Lund P D, et al. Improving the performance of a 2-stage large aperture parabolic trough solar concentrator using a secondary reflector Renewable Energy, 2020, 152(C):23-33.

[4] Zhang X, Cui Z, Zhang J, et al. Optical performance analysis of an innovative linear focus secondary trough solar concentrating system. frontiers in Energy, 2019, 13(3):590-596.

[5] Widjaja A S, K Löwe, Costa F S. Design and simulation of a concentrated solar thermal system with an integrated concrete storage for continuous heat supply. Energy Procedia, 2018, 155 (11):121-135.

[6] Zhou R, Wang R, Xing C, et al. Design and analysis of a compact solar concentrator tracking via the refraction of the rotating prism. Energy, 2022, 251(C):178-192.

[7] Dugaria S, Bortolato M, Col D D, et al. Modelling of a direct absorption solar receiver using carbon based nanofluids under concentrated solar radiation. Renewable Energy, 2018, 128(PB):495-508.

[8] Gang W A, Zhen Z A, Tj A, et al. Thermodynamic and optical analyses of a novel solar CPVT system based on parabolic trough concentrator and nanofluid Case Studies in Thermal Engineering, 2022, 33(5):101948-101965.

[9] Mihaa B, Lh A, Ys A. Advanced Modeling of Nanofluid-Based Solar Receivers in the Concentrated Solar Power Trough to Enhance the Heat Absorptivity. 2021, 7(11):901-920.

[10] Danfulani B I, Mohamed K K A, Khalil I S. BIM collaborative design: a critical perspectives of technology-supported multidisciplinary practice. Bima Journal of Science and Technology, 2024, 8(1b): 64-86.

[11] Patching A, Skitmore M, Rusch R, et al. Case study of the collaborative design of an integrated BIM, IPD and Lean university education program. International Journal of Construction Management, 2024, 24(7): 799-808.

[12] Abbas M A, Ajayi S O, Oyegoke A S, et al. A cloud-based collaborative ecosystem for the automation of BIM execution plan (BEP). Journal of Engineering, Design and Technology, 2024, 22(4): 1306-1324.

[13] Fazeli A, Banihashemi S, Hajirasouli A, et al. Automated 4D BIM development: The resource specification and optimization approach. Engineering, Construction and Architectural Management, 2024, 31(5): 1896-1922.

[14] Zhou L, Kan J, Shi J, et al. The Research on Approach of BIM-Based 3D Design for Transmission Line Project. IOP Conference Series: Earth and Environmental Science, 2021, 719(2):022006-0220014.

[15] Long R, Li Y. Research on Energy-efficient Building Design Based on BIM and Artificial Intelligence. IOP Conference Series: Earth and Environmental Science, 2021, 825(1):012003-012008.

[16] Chen J, Luo Y, Du W. Research on BIM Forward Design Based on Oblique Photogrammetry Reality Model. iOP Conference Series: Earth and Environmental Science, 2019, 267(4): 042100-142109.

[17] Mehrbod S, Staub-French S, Mahyar N, et al. Beyond the clash: investigating BIM-based building design coordination issue representation and resolution. 2019, 24 (3):33-35.

[18] Lobo J, Lei Z, Liu H, et al. Building information modelling-(BIM-) based generative design for drywall installation planning in prefabricated construction. Hindawi Limited, 2021, 2021(7):6638236. 1-6638236. 16.

[19] Lu Y, Shi L. BIM architecture design from the perspective of smart city and its application in traditional residential design. Journal of Intelligent and Fuzzy Systems, 2020, 40(12):1-10.

[20] Carnot P, Ergan S. Owner requirements in as-built BIM deliverables and a system architecture for FM-specific BIM representation. Canadian Journal of Civil Engineering, 2019, 47(2):172-186.

[21] Heaton J, Parlikad A K, Schooling J. Design and development of BIM models to support operations and maintenance. Computers in Industry, 2019, 111(4):172-186.

[22] Ma Z, Liu Z. Ontology- and freeware-based platform for rapid development of BIM applications with reasoning support. Automation in Construction, 2018, 90(JUN.):1-8.

[23] Hollberg A, Genova G, Habert G. Evaluation of BIM-based LCA results for building design. Automation in construction, 2020, 109(Jan.):102972. 1-102972. 9.

[24] Anna G, Giada M, Florian K, et al. The anti-apoptotic Bcl-2 protein regulates hair follicle stem cell function. EMBO reports, 2021, 22(10):52301-52309.

[25] Badiei Y M, Traba C, Rosales R, et al. Plasma-Initiated Graft Polymerization of Acrylic Acid onto Fluorine-Doped Tin Oxide as a Platform for Immobilization of Water-Oxidation Catalysts. ACS Applied Materials & Interfaces, 2021, 13(12):14077-14090.

[26] Alsafouri S, Ayer S K. Review of ICT Implementations for Facilitating Information Flow between Virtual Models and Construction Project Sites. Automation in Construction, 2018, 86(FEB.):176-189.

[27] Sayyad S U, Patil P V, Attar P R. Cost Comparison of a Sewage Treatment Plant Unit by Conventional Method and BIM Approach. ASEAN Engineering Journal, 2024, 14(4): 79-86.